Design, fabrication and experimental performance of seismic shear panel dampers

A.C. Wu
National Center for Research on Earthquake Engineering, Taipei, Taiwan.

K.C. Tsai, J.T. Lai, D.W. Chen, W.Y. Li, S.W. Xu
Department of Civil Engineering, National Taiwan University, Taipei, Taiwan.

ABSTRACT

A three-segment shear panel damper (SPD) consists of top and bottom elastic joints (EJs) and an inelastic core (IC) in the middle. This paper reports the seismic performance of two identical 1 m deep and 2.6 m tall specimens fabricated from using a hybrid steel wide-flange section with 30 mm SN490 steel flanges and 8 mm SN400 web. In each specimen, elastic joints are stiffened with 10 mm web doubler plates and plug welds. The only difference is in the stiffener layouts in the two 750 mm-tall IC webs. They were stiffened, meeting the proposed design procedures simplified from the model building specifications, to develop a peak shear deformation up to 0.08 and 0.13 radians, respectively. Cyclic loading tests indicate that both two SPD specimens performed remarkably well, all sustained a peak IC shear deformation larger than 0.12 radian without obvious stiffness or strength degradation. Both two specimens fractured near the fillet weld attaching the stiffener to the IC web during the first cycle of 0.15 radian shear deformation. Whilst the peak strengths of the two specimens are almost the same, all the EJs performed as intended, maintained elastic throughout the tests without any sign of yielding or instability. Applying the same design methodology, the performance of eight specimens using four different fabrication procedures is discussed. They include the use of both hot rolled or build-up wide flange wide flange members. The paper concludes with the recommendations on the design of the proposed shear panel dampers for severe seismic service.

1 INTRODUCTION

Recent researches on steel dampers have focused on providing supplemental energy dissipation for improved seismic performance. For example, from Argentina, the multiple friction damper is composed of friction elements that can be stacked around an existing column to dissipate energy (Martinez and Curadelli, 2017).

In China, the curved surfaces of the arc-surfaced frictional damper in a diagonal brace, result in damping forces that vary with displacement (Wang et al., 2017). Korean researchers have combined a steel slit damper and rotational friction dampers for seismic retrofit of a reinforced concrete moment frame (Lee et al., 2017). Using a different mechanism, the stiffness, strength and ductility of a steel moment frame can be enhanced by incorporating the shear panel dampers (SPDs) in some or all stories as shown in Figure 1. The proposed SPDs include three segments using two different steel wide-flange sections (Tsai et al., 2018). During small earthquakes, the entire SPD should remain elastic. Under strong earthquakes, the top and bottom two segments, which use the same cross-sectional properties, are designed to remain elastic while the middle segment can undergo inelastic deformations thereby dissipating seismic energy. Whilst the top and bottom segments, which use a stronger section, are named as the elastic joints (EJs), the middle segment is defined as an inelastic core (IC), which uses a thinner or weaker grade of steel than the EJs.

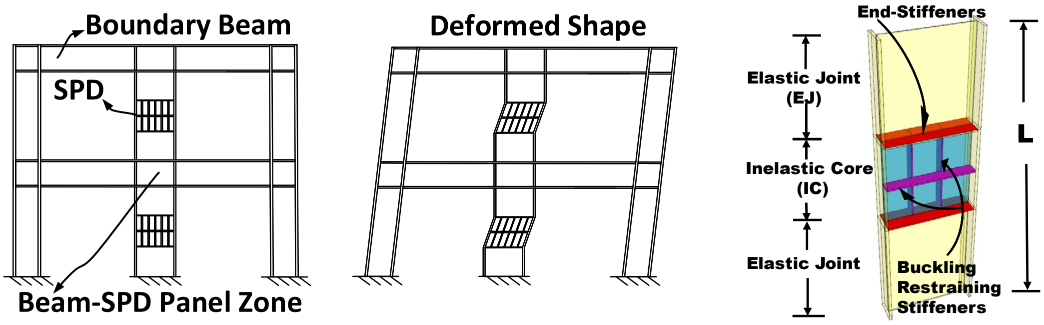

Figure 1: SPDs in a MRF and the definitions of various segments and stiffeners.

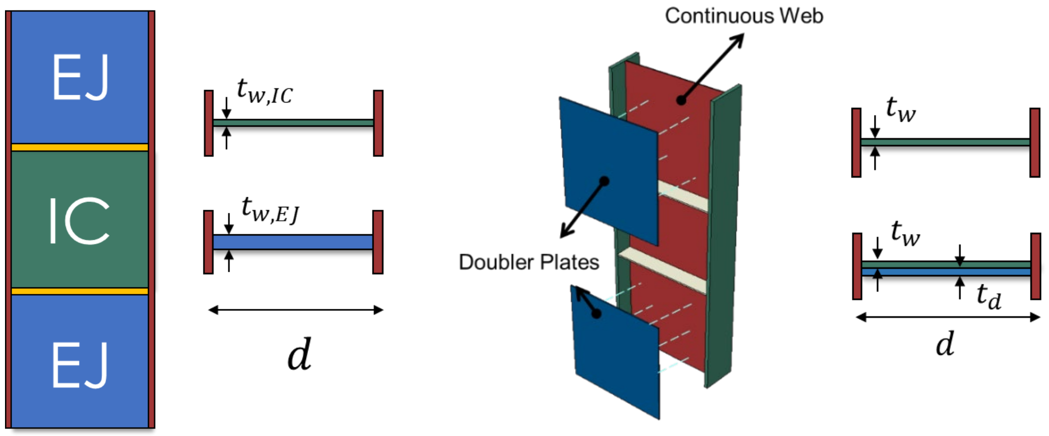

Figure 2: Three-segment SPD constructions using separate plate for the IC and EJs (left), and using a continuous web and two doubler plates (right).

The SPD must be properly portioned using capacity design principle for the flanges and EJ webs. Stiffness and strength of the proposed SPD can be decoupled (Tsai et al., 2018). The overall stiffness of a SPD with a specific shear strength can be increased, by either reducing the IC height or increasing the EJ web thickness beyond that required from the capacity design point of view. Moreover, the boundary beams, which support the SPDs from the given and adjacent stories must be properly proportion to achieve a desirable yielding mechanism (Tsai et al., 2018, Tsai and Chang, 2020). Thus, a cost-effective design can be achieved by considering the stiffness contributions from both the SPDs and the boundary beams (Tsai and Chang, 2020).

In the prior researches (Tsai et al., 2018, Tsai and Chang, 2020), the construction of SPDs adopted two continuous SN490-steel flanges, two thick SN490-steel EJ webs and one thin SN400-steel IC web. The IC web is properly stiffened with buckling-restraining stiffeners (Figure 1), whilst the three web plates must be properly cut, fitted and welded to the flanges and the end stiffeners. In fact, fabricating built-up wide-flange sections using submerged arc welding process joining the three plates is rather common in Taiwan. There could be some cost saving if a long-span wide-flange hybrid steel section can be fabricated first from two continuous SN490 flanges and one single SN400 web. Then, the SPD can be conveniently cut and fabricated from such a long member since there are likely more than one SPD with specific strength in a building construction project. After cutting, in this case the IC web is continuously extended into the EJs (Figure 2), and the EJs are strengthened beyond the dividing end-stiffener using web doubler plates. The objectives of this research are to develop and validate: (1) the capacity design procedure for the SPDs using doubler plates for the EJs; (2) a simplified design procedure for the IC web stiffeners.

2 EXPERIMENTAL PROGRAM

2.1 Design of specimens

The nominal shear strength the proposed SPD, V_y can be computed considering the shear area ($dt_{w,IC}$) of the IC and the shear yield stress (F_y) of the IC steel grade:

$$V_y = 0.6F_y dt_{w,IC} \tag{1}$$

The maximum possible strength the SPD, V_{max} can be estimated from the possible material over-strength (R_y) of the given steel grade and strain hardening (ω) of the IC web when it is undergoing large inelastic deformation:

$$V_{max} = \omega R_y V_y \tag{2}$$

Thus, the flexural demands (M_u) versus the required capacities (M_n) at the outer ends of IC and EJ can be evaluated using Equations (3) and (4) with LRFD procedures (AISC 2016) and a strength reduction factor ϕ = 0.9. Note that the IC web is not considered in computing the flexural capacity at the IC end when it is undergoing large inelastic shear deformations.

$$M_{u,IC} = \frac{V_{max} h_{IC}}{2}, M_{u,EJ} = \frac{V_{max} h_{SPD}}{2} \tag{3}$$

$$M_{u,IC} \le \phi M_{n,IC} = \phi Z_f F_{yf}, M_{u,EJ} \le \phi M_{n,EJ} = \phi(Z_f F_{yf} + Z_{w,EJ} F_{yw,EJ}) \tag{4}$$

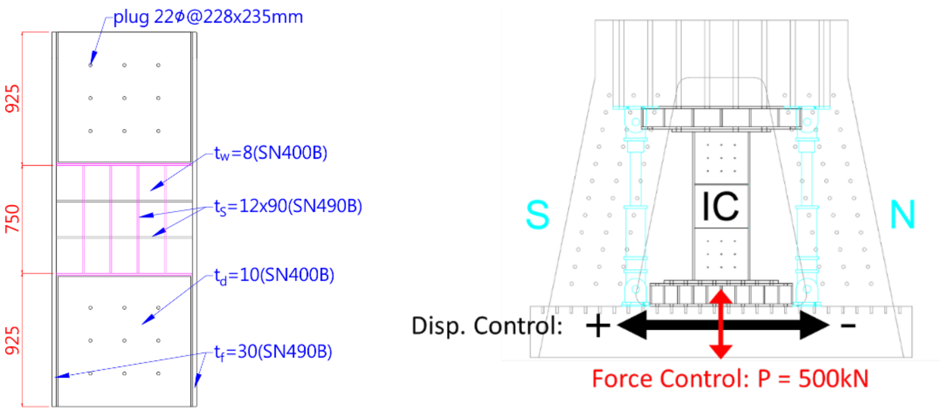

Figure 3: Dimensions of specimen SPD-4L2T and experimental setup.

Considering the load capacity of the experimental facility, the size of the full-scale specimens were designed as large and as practical possible. The overall height of the specimens 2.6 m is considered from a story height of 3.4 m and the depth of the boundary beam of 800 mm. The SPD is 1m in depth, with an 750 mm-tall IC and two 925 mm-tall EJs as shown in Figure 3. The SN490 steel (F_y = 325MPa) is considered for the 30 mm-thick flanges, whilst SN400 steel (F_y = 235MPa) is assigned for the 8 mm-thick IC web and the 10 mm-thick doubler plates in the EJs. These aforementioned sizes and steel grades meet the requirements described in Equations (1) to (4). Complete joint penetration welds (E70 electrode) were adopted to connect the IC web plate to the SPD flanges. Before the fabrication, additional Abaqus finite element model analysis results confirmed the requirements of the 10mm-thick doubler plate and the plug welds to ensure the stability of both the EJ web and the doubler plate when the IC undergoes lager inelastic deformations.

For the design of IC web stiffeners, provisions for the shear link in the eccentrically braced frames (AISC 2016) and those for SPDs (AIJ 2014) were compared. It is prescribed for the AISC shear link that web stiffeners be devised on both sides of the web transverse to the flanges, whilst stiffeners be placed transversely on one side of the web and longitudinally in the opposite side for AIJ SPDs. Both two specify the stiffeners' spacing based on the estimated peak shear deformation demands. AISC prescribes that the shear deformation demand be less than 0.08 radian. It can be found that the AIJ provisions result in an overall slightly lighter weight of stiffeners. The two-way stiffeners factually divide the entire IC web into several subpanels thereby stabilizing the entire IC to undergo large inelastic shear deformations. Both AISC and AIJ provisions prescribe the minimum thickness or stiffness of the stiffeners. In this study, design procedures of the AIJ provisions are chosen, simplified and summarized below:

(1) Calculate the depth-to-height ratio, α_s of each subpanel after deciding the number of longitudinal (n_L) and transverse (n_T) stiffeners, using the net distance $d_w = d - 2t_f$:

$$d_s = \frac{d_w}{n_L+1}, h_s = \frac{h_{IC}}{n_T+1}, \alpha_s = \frac{d_s}{h_s} \tag{5}$$

(2) Check the height-to-thickness ratio of the subpanel to meet the estimated peak shear deformation demand γ_u:

$$\frac{h_s}{t_w} \leq \sqrt{\frac{8.5k_c}{2\gamma_u - \gamma_y}}, k_c = \begin{cases} 8.98 + \frac{5.6}{\alpha_s{}^2}, \alpha_s \geq 1 \\ 5.6 + \frac{8.98}{\alpha_s{}^2}, \alpha_s < 1 \end{cases} \tag{6}$$

(3) Determine the thickness t_s and width b_s of the stiffeners considering the minimum hight-to-thickness ratio of 9.0 (AIJ 2014). Compute each stiffener's flexural stiffness I_s and the relative stiffness γ_s:

$$I_s = \frac{t_s b_s{}^3}{3}, \gamma_s = \frac{EI_s}{d_w h_{IC}} \tag{7}$$

(4) Compute the optimal relative stiffness γ_s^* considering the aspect ratio of the subpanel. Empirical Equation (8) is the regression result from this study based on an important data base (Tamai and Seo, 2014) in which the AIJ provisions are developed from. When the subpanel aspect ratio is close to 1.0, γ_s^* approaches the minimum.

$$\gamma^* = 152.7\, log(\alpha_s)^2 + 21.14\, log(\alpha_s) + 26.34 \tag{8}$$

(5) If the stiffener's stiffness ratio γ_s/γ_s^* equals to 1.0, it implies the inelastic shear buckling resistance of the subpanel and the entire IC web is about the same. It is suggested that γ_s/γ_s^* be greater than 3.0 (AIJ 2014).

Accordingly, specimens SPD-4L2T and SPD-3L4T are designed for an estimated peak shear deformation γ_u of about 0.08 and 0.13 radians, or story drift θ_u of 0.025 and 0.04 radian based on the SPD height of 2.6 m. As shown in Figure 3, 4L2T stands for the layout of the 4-longitudinal and 2-transverse stiffeners. Key specimens' dimensions are listed in Table 1. Key design parameters are given in Table 2 using the IC web nominal yield stress with R_y=1.3 and ω=1.5 for Equations (1) and (2). Note-worthy stating that the stiffness ratio γ_s/γ_s^* of SPD-3L4T is 1.2, only slightly larger 1.0. In Table 2, the values of $(h_s/t_w)_{req}$ are computed from

Equation (6) using the nominal yield stress of SN400 steel. Each end of the SPD specimens was fully welded to an end plate before anchoring into the loading apparatus.

Table 1: Dimensions of the specimens (mm).

Specimen	h	d	b_f	$t_{w,IC}$	$t_{w,EJ}$	t_f	h_{IC}	t_s	b_s
SPD-4L2T	2600	1000	250	8	8+10	30	750	12	90
SPD-3L4T								9	80

Table 2: Key design parameters of the specimens.

Specimen	V_y (kN)	V_{max} (kN)	θ_u (% rad)	γ_u (% rad)	$(h_s/t_w)_{req}$	h_s/t_w	γ_s/γ_s^*
SPD-4L2T	1128	2200	2.5	7.9	34.3	31.3	3.2
SPD-3L4T			4.0	12.9	19.4	18.8	1.2

2.2 Experimental setup, instrumentation and loading protocol

In this research, the 6-DOF multi-axial testing system (MATS) in National Center for Research on Earthquake Engineering (NCREE) is adopted as in the previous study (Tsai et al., 2018). Strong steel bearing blocks were placed on the top and bottom of the SPD specimen end plates. Post-tension rods were used on the stiffened end plates in order to securely anchor the specimen into the MATS. Various displacement transducers, strain gauges and optical displacement sensors were instrumented at each segment of the specimens. The cyclically increasing lateral displacements followed those prescribed in the model specifications for testing of welded moment connections (AISC 2016). Applying the MATS platen's longitudinal translations without introducing rotations, the in-plane target cyclic inter-story drift ratios (IDRs) are 0.125%, 0.375%, 0.5%, 0.75%, 1%, 1.5%, 2%, 3%, 4%, and 5%, each with the required number of cycles. Throughout the cyclic loading test, a constant 500 kN compression was imposed on each SPD specimen to simulate the effects of the gravity loads.

3 EXPERIMENTAL RESULTS

Tensile coupon strengths of various plates are listed in Table 3. Key force and deformation responses of the specimens are given in Figure 4 and Table 4. In the table, experimental yield strength V_{ey} is computed from the IC web plate's tensile coupon strength. The experimental ultimate IDR θ_{eu} considers the peak deformation cycle imposed on the specimens before the failure of the specimens occurred. The experimental ultimate shear deformation γ_{eu} is the peak shear deformation developed in the IC before the loading cycle where failure or strength degradation of the specimens occurred shown in Figure 4. The cumulative plastic deformation (CPD) of the IC is normalized with respect to the shear yield strain γ_y=0.0026 using τ=0.6F_y and the IC web's tensile coupon strength. In the right four columns of Table 4, experimental flexural strength $M_{en,IC}$ and $M_{en,EJ}$ are evaluated using Equation (4) with tensile coupon yield stresses of the flanges, web and doubler plates, whilst experimental flexural demands $M_{eu,IC}$ and $M_{eu,EJ}$ are computed from using experimental peak lateral force V_{emax} and Equation (3).

Test results indicate that both specimens performed remarkably well. The EJs in the two specimens performed as expected, remained elastic throughout the tests. Specimen SPD-4L2T was fabricated with a larger height-to-thickness ratio (31.3 vs. 18.8), but performed not noticeably worse, than SPD-3L4T. This should be attributed to the stiffer stiffeners (12×90 vs. 9×80 mm) adopted in the 4L2T. The requirement of the stiffness ratio be greater than 3.0 appears conservative. However, it has made SPD-4L2T to sustain cyclically increasing shear deformations well beyond the expected 0.08 radian without a strength degradation. The peak, cumulative deformational capacities, and the peak strengths of the two specimens are extraordinarily similar.

Table 3: Tensile coupon strengths of the steel plates.

Material	Grade	Thickness (mm)	F_y (MPa)	F_u (MPa)
Flange	SN490	30.2	366	523
Web	SN400	8.01	337	450
Doubler plate	SN400	10.1	354	451
Stiffener	SN490	12.1	405	525
Stiffener	SN490	9.04	285	414

Table 4: Key experimental responses of the specimens.

Specimen	V_{ey} (kN)	V_{emax} (kN)	$\frac{V_{max}}{V_y}$	θ_{eu} (% rad)	γ_{eu} (% rad)	CPD	$M_{en,IC}$	$\frac{M_{eu,IC}}{M_{en,IC}}$	$M_{en,EJ}$	$\frac{M_{eu,EJ}}{M_{en,EJ}}$	$\frac{V_{emax}}{V_{en,EJ}}$
SPD-4L2T	1618	2438	1.51	4.0	12.1	410	2324	0.39	3530	0.90	0.76
SPD-3L4T		2507	1.55	4.0	12.0	404	2324	0.40	3530	0.92	0.79

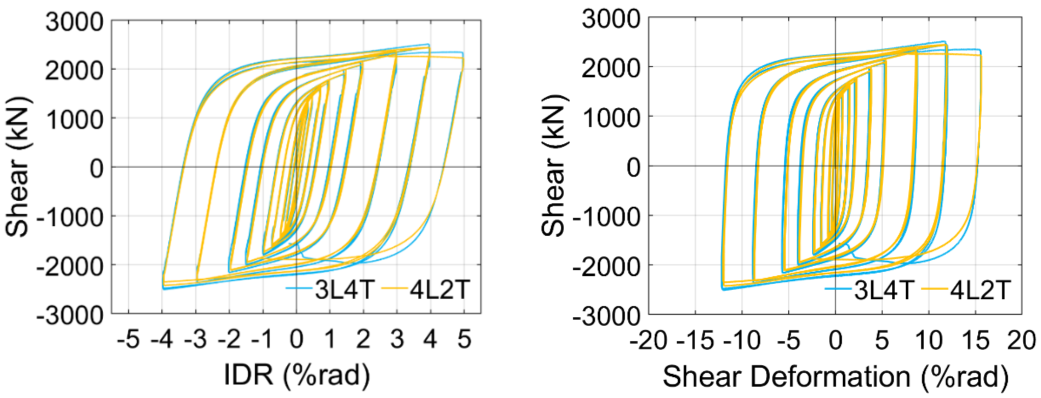

Figure 4: Experimental later force vs. deformation relationships of the specimens of the entire 2.6m-tall SPDs (left), and the 750mm-tall ICs (right).

4 CONCLUSIONS

From the tests of the two SPD specimens, conclusions can be made as follows:

(1) Properly designed and fabricated three-segment SPDs can sustain a large inelastic story drift without noticeable stiffness or strength degradation, thereby dissipating large significant amount of seismic energy.

(2) SPDs can be effectively fabricated from the proposed method using a hybrid steel beam member, dividing end-stiffeners, EJ web doubler plates and IC web buckling restraining-stiffeners. The hybrid steel beam member consists of SN400 web and SN490 flanges.

(3) Using the proposed procedures, the IC web stiffeners can be layout and proportioned to meet the specified large inelastic shear deformation demand. Test results suggest that the proposed SPD design and fabrication procedures are practical and conservative for severe seismic services.

(4) SPDs can also be fabricated using a single hot rolled wide flange member. Recent experimental and analytical studies (Chen and Tsai, 2024) have confirmed that each EJ can be made by attaching a pair of WT-shape stiffeners on the flanges of the hot rolled wide flange member. The two test specimens had excellent energy dissipation performance. The elastic lateral stiffness and maximum shear strength computed from the proposed procedures agree with the experimental results within 5%. The experimental responses of the two specimens can also be accurately simulated using Abaqus finite element model analysis.

5 REFERENCES

American Institute of Steel Construction (2016). "*Seismic Provisions for Structural Steel Buildings (341-16)*". American Institute of Steel Construction, Chicago, USA.

Architectural Institute Japan (2014). "*Design Standard for Steel Structures*". Architectural Institute Japan, Japan.

Chen WD and Tsai KC (2024). "Experimental and analytical investigation of WT-shapes stiffened steel panel dampers". *Earthquake Engineering & Structural Dynamics*, **53**(1): 23-42.

Lee J, Kang H and Kim J (2017). "Seismic performance of steel plate slit-friction dampers". *Journal of Constructional Steel Research*, **136**: 128-139.

Martinez CA and Curadelli O (2017). "Testing and performance of a new friction damper for seismic vibration control". *Journal of Sound and Vibration*, **399**: 60-74.

Tsai KC and Chang CH (2020). "Optimization of steel panel damper design for seismic moment frames". *In ICSCEA 2019: Proceedings of the International Conference on Sustainable Civil*, Ho Chi Minh City, Vietnam; 2020.

Tsai KC, Hsu CH, Li CH and Chin PY (2018). "Experimental and analytical investigations of steel panel dampers for seismic applications in steel moment frames". *Earthquake Engineering & Structural Dynamics*, **47**(6): 1416-1439.

Tamai H and Seo F (2014). "On optimum stiffener flexural rigidity ratio of shear panel damper". *Journal of Structural and Construction Engineering (Transactions of AIJ)*, **79**(706): 1983-1990.

Wang G, Wang Y, Yuan J, Yang Y and Wang D (2017). "Modeling and experimental investigation of a novel arc-surfaced frictional damper". *Journal of Sound and Vibration*, **389**: 89-100.